

SCIENTIFIC REPORTS

OPEN

Tunable exchange bias in dilute magnetic alloys – chiral spin glasses

Matthias Hudl¹, Roland Mathieu² & Per Nordblad²

Received: 06 October 2015

Accepted: 22 December 2015

Published: 28 January 2016

A unidirectional anisotropy appears in field cooled samples of dilute magnetic alloys at temperatures well below the cusp temperature of the zero field cooled magnetization curve. Magnetization measurements on a Cu(13.5 at% Mn) sample show that this anisotropy is essentially temperature independent and acts on a temperature dependent excess magnetization, ΔM . The anisotropy can be partially or fully transferred from being locked to the direction of the cooling field at lower fields to becoming locked to the direction of ΔM at larger fields, thus instead appearing as a uniaxial anisotropy. This introduces a deceiving division of the anisotropy into a superposition of a unidirectional and a uniaxial part. This two faced nature of the anisotropy has been empirically scrutinized and concluded to originate from one and the same exchange mechanism: the Dzyaloshinsky-Moriya interaction.

The unidirectional anisotropy (E_{ud}) causing exchange biased hysteresis loops in dilute magnetic alloys appears in field cooled samples at temperatures well below the cusp temperature of the zero field cooled magnetization curve¹. This anisotropy is found to have very specific characteristics: It is essentially temperature independent and acts on a temperature dependent excess magnetization (ΔM); the direction of the anisotropy field is set by the direction of the applied cooling field. The anisotropy can be partially or fully transferred from being locked to the direction of the cooling field at lower fields to becoming locked to the direction of ΔM at larger fields, thus appearing as a uniaxial anisotropy. This introduces a deceiving division of the anisotropy into a superposition of a unidirectional and a uniaxial part². In this report, this two faced nature of the anisotropy is empirically scrutinized and concluded to originate from one and the same exchange mechanism: the Dzyaloshinsky-Moriya interaction^{3,4}.

Exchange bias was first observed some 60 years ago in a field cooled system of cobalt particles with a shell of cobaltous oxide—“A new type of magnetic anisotropy has been discovered which is best described as an exchange anisotropy”^{5,6}. A similar type of anisotropy, causing shifted hysteresis loops, occurs in certain dilute magnetic alloys, and has been extensively investigated in Cu(Mn) alloys of different manganese concentration^{7–13}. Atomic short range order¹⁴ and induced inhomogeneity may affect the hysteresis behavior of Cu(Mn) alloys as demonstrated by Monod *et al.* in Figure 8 of Ref. [10] by measurements on a cold worked sample. Such defects are revealed by severe broadening of the low field maximum of the zero field cooled (ZFC) magnetization vs. temperature curve and enhanced temperature for the onset of irreversibility between the ZFC and field cooled (FC) magnetization curves¹⁵. Exchange bias also occurs in bilayers of a ferromagnetic and an antiferromagnetic material and such structures have contributed to the continuously increased storage capacity in magnetic hard discs; being used as key components of both the read head and the storage medium. However, the physical mechanisms behind exchange bias are yet of unsettled origin and remain a scientific controversy¹⁶. Of special interest in the context of the current investigation is the exchange bias effect reported on a bilayer of spin glass, Cu(Mn 6 at%), and cobalt layers¹⁷.

Figure 1(a) shows field cooled (FC) hysteresis loops of our Cu(13.5 at% Mn) (hereafter referred to as CuMn) sample measured in different cooling fields, H_{FC} at the temperature $T_m = 5$ K or reduced temperature $T_m/T_g = 0.09$ (the spin glass temperature of the sample is $T_g = 57$ K¹⁸). All hysteresis loops are measured in-between the maximum fields $\pm H_{FC}$. Three characterizing parameters can be extracted from these curves: An excess moment, ΔM , a first switch field H_{sw1} and a second switch field H_{sw2} as defined in Fig. 1(b). The variation of these parameters with the magnitude of the cooling field is plotted in the insets of Fig. 1(a). Figure 1(b) shows a full hysteresis loop of the CuMn sample measured up to a maximum field of 14 T. The initial branch of the hysteresis loop has a characteristic S-shape without sudden magnetization jumps. The first decreasing branch of the hysteresis loop shows a sharp jump, defining ΔM , at the switch field, H_{sw1} , and on the following field increasing branch of the hysteresis loop, a magnetization reversal of the same magnitude ΔM occurs in the opposite direction at the switch field

¹Stockholm University, Department of Physics, Chemical Physics, SE-106 91 Stockholm, Sweden. ²Uppsala University, Department of Engineering Sciences, Solid State Physics, Box 534, SE751 21 Uppsala, Sweden. Correspondence and requests for materials should be addressed to P.N. (email: per.nordblad@angstrom.uu.se)

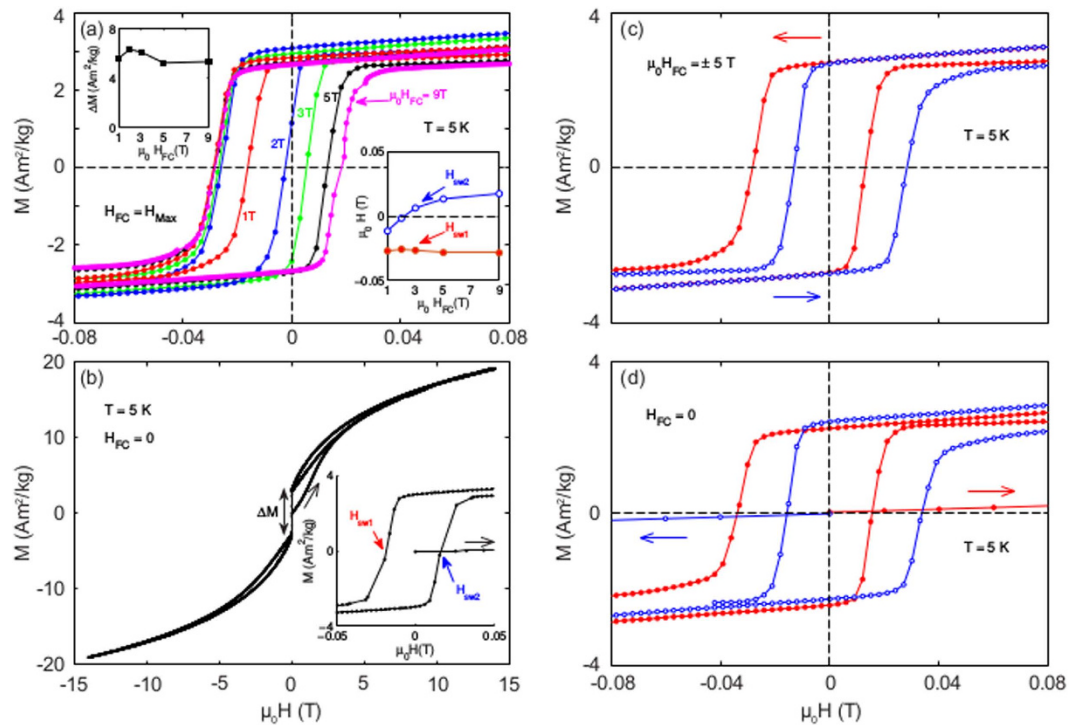


Figure 1. Magnetic hysteresis and tunable exchange bias. (a) The central part of M vs. H loops after cooling the sample in H_{FC} to 5 K, and measure the hysteresis loop on decreasing the field to $-H_{FC}$ and back to $+H_{FC}$. The insets show the field dependence of the parameter H_{sw1} , H_{sw2} , (right) and ΔM (left) in the H_{FC} range 1 to 9 T. (b) Full hysteresis loops measured at 5 K from 0 to 14, 14 to -14 and then back $+14$ T. The inset shows the central part of the loop and the fields H_{sw1} and H_{sw2} are marked. The jump and definition of the excess magnetization, ΔM , is indicated in the main frame. (c,d) The central part of the hysteresis loops measured after field cooling (c) and zero field cooling (d) in fields up to 5 T at 5 K. The arrows indicate the initial field sweep direction. (Red loops - positive initial fields, blue loops - negative initial fields).

H_{sw2} . As is seen in Fig. 1(a), ΔM and H_{sw1} are both essentially independent of the cooling field strength in the considered field range (1 to 9 T). H_{sw2} , on the other hand, starts out from a value rather close to H_{sw1} and continuously increases with increasing H_{FC} to asymptotically approach the value $-H_{sw1}$ at very high fields. The three parameters are weakly dependent on repeated hysteresis measurements (training) as long as the maximum field of the loops does not exceed the initial cooling field. However, if the maximum field, H_{max} of the hysteresis measurement is increased, H_{sw2} shifts to the same value as observed after field cooling in H_{max} , whereas ΔM and H_{sw1} remain essentially unaffected by the field increase. Using the product of ΔM and H_{sw1} one can derive a measure of the anisotropy energy related to the switching of the excess magnetization ΔM . This anisotropy, $E_{udT} \propto \Delta M H_{sw1}$, is independent of the magnitude of the cooling field. Looking at the field dependence of H_{sw2} , one observes that at low cooling fields, the anisotropy of the sample is near unidirectional ($H_{sw1} \sim H_{sw2}$), and that with increasing cooling field it attains the mentioned mixed unidirectional/uniaxial character² and finally striving towards only a uniaxial character at very high fields. Figure 1(c) shows hysteresis loops after field cooling in $+5$ T and -5 T, and Fig. 1(d) shows hysteresis loops measured after zero field cooling (ZFC) and first applying the field up to 5 T in subsequently the positive and the negative direction. Remarkably, both the FC and the ZFC protocols reveal similarly exchanged biased ($H_{cb} = (H_{sw1} + H_{sw2})/2$) hysteresis loops.

The field controlled two-faced character of the anisotropy: unidirectional and uniaxial, may be explained by the exchange mechanism giving rise to anisotropy in a Heisenberg spin system: the Dzyaloshinsky-Moriya interaction (DMI)^{3,4} and the chirality¹⁹ of the local spin structure (see also Levy *et al.*² and Staunton *et al.*^{20,21}). Only a weak cooling field introduces one polarity of the chiral spin structures yielding unidirectional anisotropy along the field direction. This anisotropy acts on the excess magnetization, which switches when the applied magnetic field exceeds H_{sw1} . This field remains independent of the strength of the cooling field. However, on field reversal, the switching field H_{sw2} is dependent on the cooling field. This behavior requires that polarity of the chirality of parts of the local spin structure switches with the excess magnetization instead of only being confined to the original cooling field direction and that the fraction of spin chirality following the switching of the excess moment is set by the magnitude of the cooling field. Using this two-faced picture of the local spin structure (locked to the cooling field direction at low fields and locked to the switching excess magnetization at high fields), only the DMI is required to explain the observed behavior and tuning of the exchange bias. At constant low temperature, the only way to change the partition between these two fractions is to apply a higher maximum field than the employed cooling field. The magnitudes of the two fractions of the DMI can be experimentally derived using the postulation that: $E_{udT} = E_{uds} + E_{udM}$, where E_{uds} denotes the part of the anisotropy that remains locked to

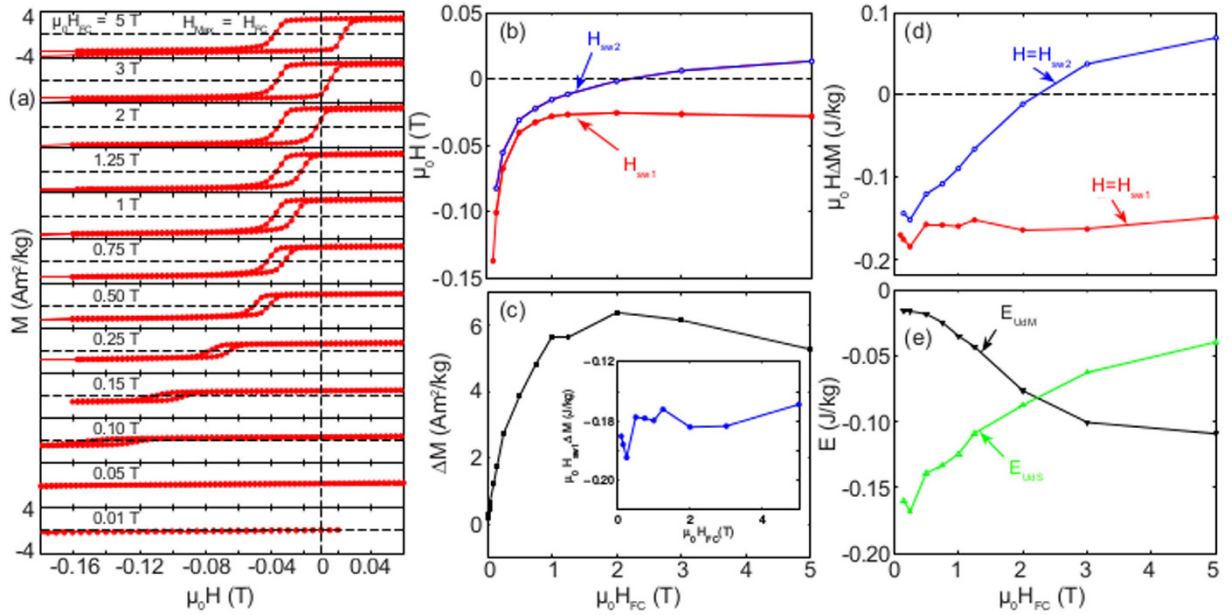


Figure 2. FC Hysteresis loops at different fields. (a) The central part of M vs H loops measured at 5 K after cooling in H_{FC} (of strength indicated in the figure) and measured in-between $\pm H_{FC}$. When $H_{FC} < 0.15$ T; the loops have been recorded up to fields high enough to reach H_{sw1} when measurable. The scale on the magnetization axes is always drawn between ± 4 Am²/kg. (b) Anisotropy fields and excess magnetization. (c) Cooling field dependence of H_{sw1} and H_{sw2} (upper panel), and ΔM (lower panel) derived from the M vs. H curves in (a). The inset shows the field dependence of the corresponding anisotropy energy $\mu_0\Delta MH_{sw1}$. (d,e) The energy $\mu_0\Delta MH$, with $H = H_{sw1}$ and H_{sw2} (d), and the energies E_{uds} and E_{udM} (e) as a function of the cooling field μ_0H_{FC} .

the direction of the cooling field and E_{udM} the part of the anisotropy that is locked to the direction of the excess moment. The two parts are then be derived from the experimental parameters through:

$$E_{udT} = \mu_0 \Delta MH_{sw1} \tag{1}$$

$$E_{uds} - E_{udM} = \mu_0 \Delta MH_{sw2} \tag{2}$$

Figure 2(a) shows the hysteresis behavior after field cooling in fields varying from 0 to 5 T and measuring hysteresis loops in fields from $+H_{FC}$ to $-H_{FC}$. From these curves the detailed behavior of the field dependence of the characterizing parameters, including the low field region between 0 and 1 T where ΔM remains unsaturated, is derived. In Fig. 2(b), H_{sw1} and H_{sw2} are plotted versus the cooling field strength and in Fig. 2(c) the corresponding dependence of ΔM is shown. From these data, the related energy measures can be derived and these are plotted in Fig. 2(d,e) showing $\mu_0\Delta MH_{sw1}$ (E_{udT}) and $\mu_0\Delta MH_{sw2}$ versus cooling field in Fig. 2(d) and the unidirectional energies E_{uds} and E_{udM} in Fig. 2(e). It is worth noting that the magnitude of the unidirectional anisotropy appears independent of cooling field strength, confirming that already an infinitesimally small cooling field is capable of aligning the polarity of the chirality in the field direction.

The temperature dependence of the hysteresis loops measured after field cooling in 1 T are shown in Fig. 3(a) and the derived parameters in Fig. 3(b,c). It is remarkable that the derived magnitude of the anisotropy energy E_{udT} also appears temperature independent. Noteworthy is also that a larger and larger part of the anisotropy becomes locked to the excess magnetization with increasing temperature. At higher temperatures than 25 K, the collective excess moment ΔM has already relaxed to zero on the time scale of these hysteresis experiments.

Our results imply that a rigid spin structure defining the anisotropy is imprinted in the spin glass on cooling to low temperatures and that only a weak field is required to establish the full strength of the unidirectional anisotropy (E_{udT}) along the direction of the applied field. The only way to alter this structure and the associated anisotropy at constant temperature is to apply a larger field (H_{max}) than the original cooling field. The effect of H_{max} is then to imprint a compensating unidirectional anisotropy that switches direction with ΔM and yields an anisotropy field that is controlled by H_{max} . It is in this context important that in a zero field cooled sample a large field is required to establish any anisotropy and excess magnetization and that the full strength of the anisotropy is only achieved at field larger than the field where the thermoremanent magnetization (TRM) and isothermal remnant magnetization (IRM) coalesce²². In this connection it is worth noting that the existence of exchange bias after zero field cooling in Heisenberg spin glasses is uncharacteristic to most other exchange bias systems, however, large exchange bias has been observed by A. K. Nayak *et al.*²³ after zero field cooling of a Mn₂PtGa Heusler alloy. This exchange bias is assigned to induced exchange coupling between ferromagnetic clusters dispersed in a

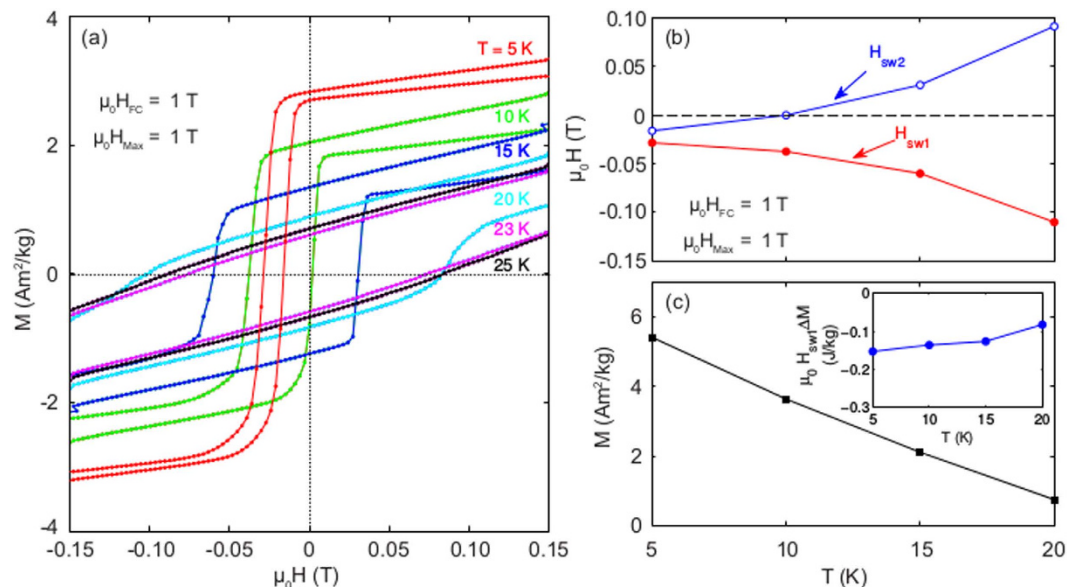


Figure 3. Temperature dependence of the hysteresis. (a) Temperature dependence of the central part of hysteresis loops measured after field cooling in $H_{FC} = 1$ T and recording the loops up to $H_{max} = \pm 1$ T. (b) Temperature dependence of H_{sw1} and H_{sw2} derived from (a). (c) The temperature dependence of ΔM and the inset shows the derived anisotropy $\mu_0 \Delta M H_{sw1}$ vs. temperature.

ferrimagnetic matrix when the sample is first magnetized at low temperature. Thus, a very different mechanism from the one discussed here for Heisenberg spin glasses.

The possibility to imprint a rigid spin structure in spin glasses that withstands significant perturbations is also manifested in low-field experiments on ageing-related phenomena showing memory of an aged spin structure at a specific temperature in spite of an apparent rejuvenation on temperature perturbations^{24–26}. Two recent reviews of J. A. Mydosh²⁷ and H. Kawamura and T. Taniguchi²⁸ comprehensively recall the remarkable physical properties of spin glass systems including discussions on the importance of the chirality in Heisenberg systems.

Methods

The sample is a polycrystalline cylinder of Cu(13.5 at% Mn) of height 5 mm and diameter 2 mm with a spin glass temperature of 57 K¹⁸. The material is prepared by the drop synthesis method²⁹. The global homogeneity and composition have been ascertained by EDS (Energy Dispersive Spectroscopy) measurements on different spots of the surface area of the sample and by the sharpness of the spin glass transition at low applied magnetic fields. Fig. S1 (in the supplementary information) shows the temperature dependence of the ZFC and FC susceptibility (M/H) of the sample at different applied fields. The experiments are performed in a Quantum Design MPMS XL SQUID magnetometer (5 T) and two different PPMS VSM systems (9 T and 14 T). All hysteresis measurements are performed after cooling the sample from a reference temperature, $T_{REF} = 70$ K.

References

1. Cannella, V. & Mydosh, J. A. Magnetic ordering in gold-iron alloys. *Phys. Rev. B* **6**, 4220–4237 (1972).
2. Levy, P. M., Morgan-Pond, C. & Fert, A. Origin of anisotropy in transition metal spin glass alloys. *J. Appl. Phys.* **53**, 2168–2173 (1982).
3. Dzyaloshinsky, I. A thermodynamic theory of “weak” ferromagnetism of antiferromagnetics. *J. Phys. Chem. Solids* **4**, 241–255 (1958).
4. Moriya, T. New mechanism of anisotropic superexchange interaction. *Phys. Rev. Lett.* **4**, 228–230 (1960).
5. Meiklejohn, W. H. & Bean, C. P. New magnetic anisotropy. *Phys. Rev.* **102**, 1413–1414 (1956).
6. Meiklejohn, W. H. & Bean, C. P. New magnetic anisotropy. *Phys. Rev.* **105**, 904–913 (1957).
7. Kouvel, J. S. Exchange anisotropy in Cu-Mn and Ag-Mn alloys. *J. Appl. Phys.* **31**, 142S–147S (1960).
8. Knitter, R. W., Kouvel, J. S. & Claus, H. Magnetic irreversibility and metastability in Cu-Mn. *J. Magn. Magn. Mater.* **5**, 356–359 (1977).
9. Beck, P. A. Properties of mictomagnets (spin glasses). *Progr. Mater. Sci.* **23**, 1–49 (1978).
10. Monod, P., Préjean, J. J. & Tissier, B. Magnetic hysteresis of CuMn in the spin glass state. *J. Appl. Phys.* **50**, 7324–7329 (1979).
11. Préjean, J. J., Joliclerc, M. J. & Monod, P. Hysteresis in CuMn: The effect of spin orbit scattering on the anisotropy in the spin glass state. *J. Physique* **41**, 427–435 (1980).
12. Felten, G. & Schwink, C. Magnetic anisotropy of CuMn spin glasses. *J. Magn. Magn. Mater.* **54–57**, 218–220 (1986).
13. Barnsley, L. C., MacA Gray, E. & Webb, C. J. Asymmetric reversal in aged high concentration CuMn alloy. *J. Phys.: Condens. Matter* **25**, 086003 (2013).
14. Schönfeld, B., Paris, O., Kostorz, G. & Skov Pedersen, J. Magnetic small-angle scattering from Cu-17 At. % Mn. *J. Phys.: Condens. Matter* **10**, 8395–8400 (1998).
15. Chamberlin, R. V., Hardiman, M. & Orbach, R. Reversibility and time dependence of the magnetization in Ag:Mn and Cu:Mn spin glasses. *J. Appl. Phys.* **52**, 1771–1772 (1981).
16. Noguees, J. *et al.* Exchange bias in nanostructures. *Phys. Rep.* **422**, 65–117 (2005).

17. Ali, A. *et al.* Exchange bias using a spin glass. *Nature Mater.* **6**, 70–75 (2007).
18. Mathieu, R., Hudl, M. & Nordblad, P. Memory and rejuvenation in a spin glass. *EPL* **90**, 67003 (2010).
19. Kawamura, H. Chiral ordering in Heisenberg spin glasses in two and three dimensions. *Phys. Rev. Lett.* **68**, 3785–3788 (1992).
20. Staunton, J. B., Gyorffy, B. L., Poulter, J. & Strange P. A relativistic RKKY interaction between two magnetic impurities – the origin of a magnetic anisotropy effect. *J. Phys. C: Solid State Phys.* **21**, 1595–1611 (1988).
21. Staunton, J. B., Gyorffy, B. L., Poulter, J. & Strange P. The relativistic RKKY interaction, uniaxial and unidirectional magnetic anisotropies and spin glasses. *J. Phys.: Condens. Matter* **1**, 5157–5163 (1989).
22. Bouchiat, H. & Monod, P. Remanent magnetization properties of the spin glass phase. *J. Magn. Magn. Mater.* **30**, 175–191 (1982).
23. Nayak, A. K. *et al.* Large zero-field-cooled exchange-bias in bulk Mn₂PtGa. *Phys. Rev. Lett.* **110**, 127204 (2013).
24. Nordblad, P. & Svedlindh, P. In *Series on Directions in Condensed Matter Physics: Vol. 12 Spin Glasses and Random Fields* (ed. Young, A. P.) Ch. 1, 1–27 (World Scientific, 1997).
25. Jonason, K. Vincent, E., Hammann, J., Bouchaud, J.-P. & Nordblad, P. Memory and chaos effects in spin glasses. *Phys. Rev. Lett.* **81**, 3243–3246 (1998).
26. Mathieu, R., Jonsson, P., Nam, D. N. H. & Nordblad, P. Memory and superposition in a spin glass. *Phys. Rev. B* **63**, 092401 (2001).
27. Mydosh, J. A. Spin glasses: redux: an updated experimental/materials survey. *Rep. Progr. Phys.* **78**, 052501 (2015).
28. Kawamura, H. & Taniguchi, T. In *Handbook of Magnetic Materials 24* (ed. Buschow K. H. J.) Ch. 1, 1–137 (Elsevier, 2015).
29. Carlsson, B., Gölin, M. & Rundqvist, S. Determination of the homogeneity range and refinement of the crystal structure of Fe₂P. *J. Sol. State Chem.* **8**, 57–67 (1973).

Acknowledgements

Financial support from the Swedish Research Council and the Göran Gustafsson Foundation is acknowledged. We thank Y. Taguchi and Y. Tokura for letting us use their 14 T PPMS system and S.A. Ivanov for EDS analyses.

Author Contributions

M.H. planned and performed the experiments and jointly wrote the final manuscript. R.M. planned and performed the experiments and jointly wrote the final manuscript. P.N. took part in planning the experiments, drafted the first version of the manuscript and jointly wrote the final manuscript.

Additional Information

Supplementary information accompanies this paper at <http://www.nature.com/srep>

Competing financial interests: The authors declare no competing financial interests.

How to cite this article: Hudl, M. *et al.* Tunable exchange bias in dilute magnetic alloys – chiral spin glasses. *Sci. Rep.* **6**, 19964; doi: 10.1038/srep19964 (2016).



This work is licensed under a Creative Commons Attribution 4.0 International License. The images or other third party material in this article are included in the article's Creative Commons license, unless indicated otherwise in the credit line; if the material is not included under the Creative Commons license, users will need to obtain permission from the license holder to reproduce the material. To view a copy of this license, visit <http://creativecommons.org/licenses/by/4.0/>